PHYSICAL REVIEW B VOLUME 21, NUMBER 8 15 APRIL 1980

Optical properties of Au: Sample effects

D. E. Aspnes, E. Kinsbron, and D. D. Bacon
Bell Laboratories, Murray Hill, New Jersey 07974
(Received 11 July 1979)

Reported optical data for Au are investigated to determine the origin of their differences. A single-parameter model representing voids in an otherwise homogeneous medium is shown to account for the major discrepancies in the above-band-gap ($E > 2.5$ eV) ϵ_2 spectra for Au samples prepared in different ways. Ellipsometric measurements on transmission-electron-microscopy (TEM) characterized thin-film samples on an energy range of 1.5–5.8 eV support the void model but show the importance of measuring both ϵ_1 and ϵ_2 to separate volume from surface film effects. Differences in below-band-gap data arise from at least two mechanisms: grain-size effects in samples with a large volume fraction of imperfections, and increased surface scattering, probably from thermal grooving, in annealed samples. Two mechanisms are required because the lowest values of ϵ_2 in the Drude region are shown to occur for unannealed but smooth, moderately thick film samples evaporated on room-temperature substrates. Our best below-band-gap data, taken on electron-beam evaporated samples, show directly the linearly increasing d-band to Fermi-level transition threshold near X at 1.8 eV unobstructed by the Drude tail. These data have an ϵ_2 value at 1.5 eV equal to within experimental error to that calculated from the scattering lifetime derived from the known resistivity of the bulk metal, indicating a grain size and quality better than anything previously used for optical measurements in Drude region.

I. INTRODUCTION

The optical properties of Au have been studied extensively by reflectance,[1–10] combined reflectance and transmittance,[11–16] and ellipsometry[4,17–28] measurements on unannealed[5,6,11,15,16,18–20,22,23,26] and annealed[1,2,8–10,13–15,19,21,24,25,27] thin-film,[4,7,13–15] thick-film,[1–4,8–10,16,18–20,22,23,26,27] and bulk[5,6,17,21,24,25] samples. Differences among these spectra, of the order of ±15% in the peak value of ϵ_2 near 3.8 eV, have been recognized and have been attributed to various effects such as roughness,[14,24,29] surface films,[5] unspecified internal electron-scattering defects,[1,2,4,14,26] strain,[1,2,24] grain-boundary material,[24,28,30,31] and voids.[8]

By contrast to the large amount of effort directed toward measuring the dielectric properties of Au, there has been very little work to understand quantitatively the discrepancies on a systematic basis for samples prepared intentionally to obtain the "best" dielectric-function data. (We exclude here investigations on pathological samples prepared specifically to study theories of the dielectric properties of heterogeneous media.[32]) The most comprehensive discussions to date are those by Thèye[14] and by Winsemius, Lengkeek, and Van Kampen.[24] While both groups attribute variations in ϵ_2 in the Drude free-electron region below about 2.5 eV to surface roughness, Thèye suggests in addition that impurity scattering is also important and that changes in the interband region above 2.5 eV are due to strain.

Our interest in optical studies of adsorption processes on metal films, which require accurate dielectric-function data, and in enhanced surface Raman scattering, which in some models[33] is attributed to surface roughness, has led us to reexamine the optical properties of Au samples prepared in different ways. If systematic differences could be identified and understood, then better, or at least better characterized and more reproducible, samples could be obtained. Moreover, the results should be applicable to other metals, which tend to show even larger differences in reported optical spectra than Au.[34]

Our conclusions can be summarized as follows. Values of ϵ_2 in the Drude region are affected primarily by grain size in poorly prepared unannealed samples, and by surface roughness in annealed samples. Surprisingly, the "best" (i.e., lowest) values of ϵ_2 in this spectral region are obtained from high-quality *unannealed* samples, even though transmission-electron-microscopy (TEM) measurements show that these samples have a smaller grain size and analysis of interband optical data shows that they contain a few percent higher volume fraction of voids than annealed samples. In fact, our best unannealed samples, which were moderately thick ($d \cong 1500$ Å) films prepared by electron beam evaporation onto NaCl or glass substrates held at room temperature, clearly show the linearly rising absorption associated with d-band to Fermi-level transitions near X unobstructed by the Drude tail, as calculated theoretically by Guerrisi, Rosei,

and Winsemius.[25] The threshold itself is determined to be 1.84± 0.02 eV. These samples have an ϵ_2 value at 1.5 eV that is equal within experimental uncertainty to that calculated from the known resistivity of the bulk metal,[35] suggesting a sample quality in the Drude region higher than previously attained in optical measurements.

In the interband region above 2.5 eV, the most important single factor affecting ϵ is not the grain size or surface roughness, but voids. We find that the major discrepancies in all reported ϵ_2 data above 2.5 eV can be described entirely by a one-parameter effective medium model that assumes the samples to contain a small volume fraction of voids, as opposed to the strain hypothesis.[14,24] For this reason, the best (i.e., highest) values of ϵ_2 in this spectral region are obtained on *annealed* samples, whose large grain size and small void concentration provide more polarizable material per unit volume. If ϵ_1 data are also considered, then an allowance for surface films may also be required. A surface film in this context can also mean a rough surface described as an effective-medium overlayer.

The outline of the paper is as follows. Experimental details of sample preparation and characterization for new spectra reported here are summarized in Sec. II. General characteristics of the dielectric-function data for Au are discussed in Sec. III A. The mathematical modeling of the effect of voids, surface roughness, and surface films on the measured dielectric function is given in Sec. III B. The above-band-gap results are discussed in Sec. III C, and the below-band-gap results are treated in Sec. III D. A discussion of the results in terms of implications for sample preparation is given in Sec. IV.

II. EXPERIMENTAL

To aid in identifying effects of sample preparation, a number of Au thin-film samples of the order of 500–5000 Å thick were prepared from 99.999% Au source material by dc getter sputtering[36] in partial pressures of Ar^+ or by electron beam evaporation onto substrates held at various temperatures. The best films, as defined by their dielectric response discussed in Sec. III, were prepared by electron beam evaporation at deposition rates of 1400 Å/min onto cleaved NaCl or glass substrates whose temperatures were less than 50 °C. The source-target separation was 30 cm, and the base pressure of 4×10^{-7} Torr typically increased to 3×10^{-6} Torr at the end of the deposition cycle. Sputtered films were prepared at 100 Å/min. or 750 Å/min. rates, for which voltage, current, power, and pressure conditions were 1000 V, 2 mA, 2 W, and 1×10^{-4} Torr and 1500 V, 10 mA, 15 W, and 1.8×10^{-4} Torr, respectively.

For a given temperature, the best sputtered films were obtained on cleaved NaCl substrates, followed in order of quality by SiO_2, glass, and sapphire. The superiority of air cleaved NaCl substrates is easy to understand because the films grow epitaxially on them.[37] Striations from imperfect cleavage regions did not affect the ellipsometric measurements used to determine the optical properties because the scattered light arising from these regions was rejected by the large f number of the instrument. Fused quartz appeared to be superior to lime glass as a substrate for reasons probably related to homogeneity of the material. The sapphire substrates were rough and nonscattering films could not be obtained on them. Representative thin films (~500 Å) deposited onto NaCl were examined for structure and homogeneity by TEM.

The dielectric functions were measured from 1.5–5.8 eV using an automatic rotating-analyzer ellipsometer (RAE) described previously.[38] The runout errors of the polarizer and analyzer in straight through operation were less than ±0.02°, a figure which also includes possible errors from residual polarization sensitivity of the photomultiplier detector. These errors produce relative changes of less than 3×10^{-4} in the dielectric function data and hence were completely negligible compared to differences due to sample preparation. A more serious source of error with the RAE itself was the uncertainty in determining the ac to dc amplitude ratio below 2 eV, where the rejection of the deflected beam in the quartz Rochon analyzer occasionally became marginal, especially if the samples showed any tendency to scatter light. However, in no case did the error exceed one percent above 2.5 eV. The uncertainties below 2.5 eV were wavelength dependent and are indicated where relevant. By correcting[39] for optical activity in the quartz Rochon prisms, and by recalibrating the instrument for each sample, other systematic errors were held to well under 1%. Thus, differences in the new spectra reported here can be attributed to genuine differences among samples and not to measurement artifacts.

III. RESULTS AND DISCUSSION

A. Data

Data from a number of recent, commonly cited sources are summarized in Fig. 1. These data include those obtained by combined reflectance and transmittance[14,15] and ellipsometric[21,25] spectro-

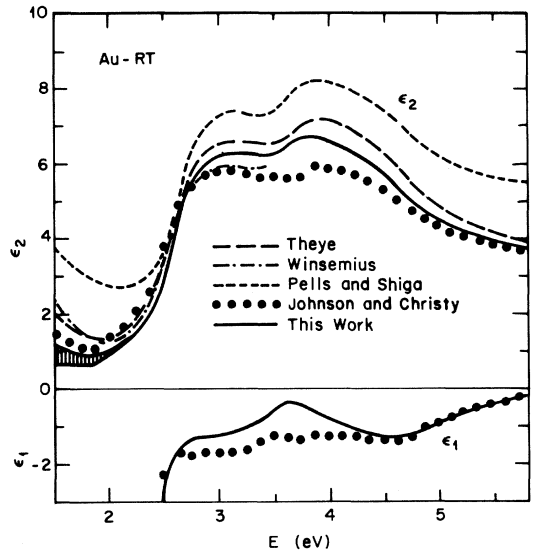

FIG. 1. Representative dielectric-function data for Au: Thèye (Ref. 14), thin film, UHV evaporated and annealed; Winsemius (Ref. 25), bulk polycrystal, UHV annealed; Pells and Shiga (Ref. 21), as Winsemius; Johnson and Christy (Ref. 15), unannealed thin film; this work, electron-beam evaporated thin film.

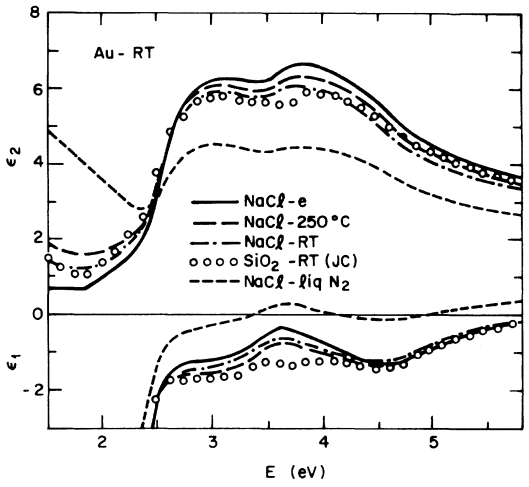

FIG. 2. Dielectric function data for sputter-deposited thin films [250° C, room-temperature (RT), liquid N_2] and a moderately thick electron-beam evaporated film (*e*) compared to the unannealed-thin-film data of Johnson and Christy (JC; Ref. 15).

scopies on unannealed[15] or annealed[14,21,25] thin-film[14,15] or bulk[21,25] samples measured in air[15] or ultrahigh vacuum,[14,21,25] and thus provide a fairly wide but representative picture of typical variations encountered. All recent data taken with the intent to measure ϵ accurately fall within the ±15% 5.9–8.1 range of peak heights in ϵ_2 shown here. ϵ_1 data usually are not provided but are given where available. Also shown in Fig. 1 are our "best" Drude-region data, taken on moderately thick ($d \sim 1500$ Å) samples electron beam evaporated onto substrates held at room temperature. The shaded band represents the wavelength dependent uncertainty discussed in Sec. II. However, the lower limit of this band is an actual spectrum taken on a sample evaporated onto a glass substrate.

Figure 2 shows further data that were obtained on relatively thin ($d \sim 500$ Å) films Ar^+ getter sputtered onto NaCl substrates held at liquid-nitrogen temperature, room temperature (RT), or 250 °C. TEM micrographs of these films are shown in Fig. 3. The liquid-N_2 sample is full of voids and defects. The projected clear area of 12% for this film is a lower bound to the actual void volume fraction, since other voids are incorporated into the three-dimensional structure. By contrast, the RT and 250 °C samples are relatively closely packed and differ mainly in grain size. The RT sample is fine grained, while the sample grown at 250 °C has a much larger average grain size owing to annealing during growth. It can be anticipated from Fig. 3 that the fine grained RT sample will have a smoother surface, and that the large grained 250 °C sample will be more densely packed. The optical data show this, as will be discussed.

The variation of the data of Fig. 2 with growth temperature follows well that of the data of Köster and Stahl[19] with annealing temperature, who however did not correlate their results with TEM measurements. We have included in Fig. 2 the Johnson-Christy[15] data on unannealed thin film samples deposited at room-temperature to show that their ϵ_2 values, low by comparison with the annealed data of Fig. 1, agree quite well with our RT data. This is expected if sample preparation, and not measurement technique, is the significant factor.

Ideally, all data should be analyzed over the entire accessible spectral region by standard linear regression analysis techniques[40] using a model consisting of a few energy-independent parameters such as Drude relaxation time, bulk void fraction, surface void fraction, and surface layer thickness. This approach was discussed previously for amorphous Si films[41] and semiconductor-oxide systems.[42] But this method requires dielectric function data for Au of a quality not presently available. Therefore, we will treat separately the free-electron and interband regions, limiting our analysis to identifying the principal mechanisms by which the data differ in each region.

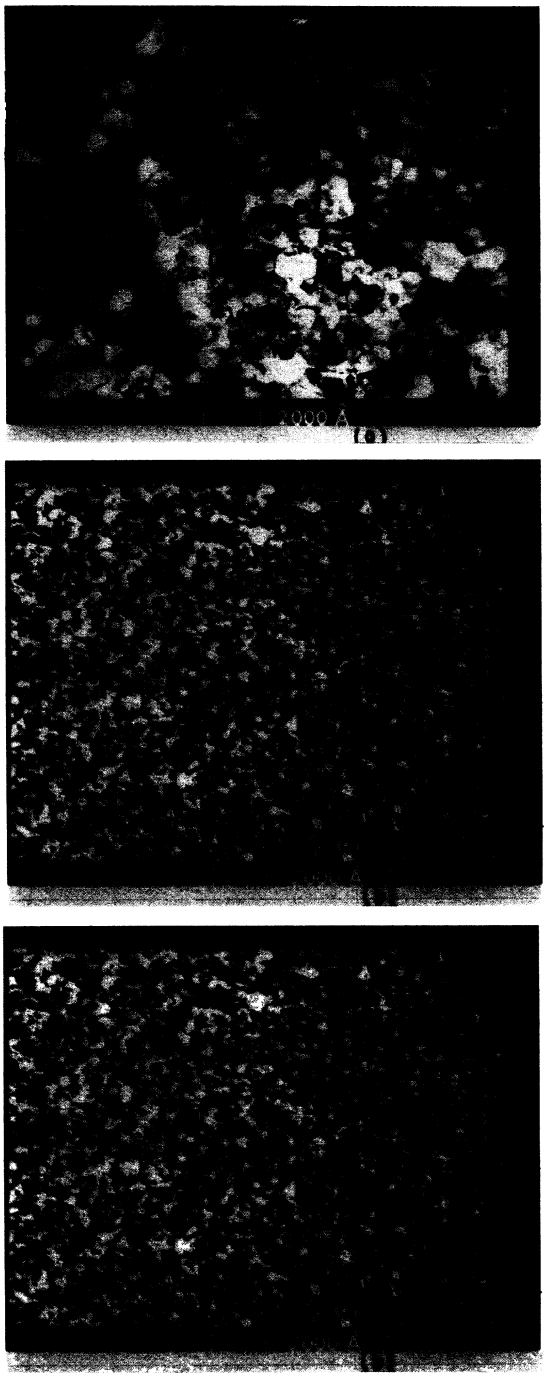

FIG. 3. TEM micrographs of sputter-deposited thin films whose dielectric function data are shown in Fig. 2. (a) 250 °C; (b) RT; (c) liquid N_2.

B. Theory

We summarize in this section the theoretical description of three principal factors that affect the actual measured, apparent or pseudo, dielectric function: surface roughness, dielectric overlayers, and voids. Their effects are qualitatively different, but can be described by combining heterogeneous dielectric theory[43-45] with standard n-phase models[46] expressing the complex reflectance ratio of a multilayer stack. The enhancement of the Drude tail in ϵ_2 by increased scattering is not contained in the model but will be discussed in Sec. III D.

We consider voids first. If ϵ is the dielectric function of Au in its homogeneous form, then the effective dielectric function, $\langle\epsilon\rangle$, of the heterogeneous material containing a volume fraction, f_V, of voids is given approximately by solving[41]:

$$\frac{\langle\epsilon\rangle-\epsilon_H}{\langle\epsilon\rangle+2\epsilon_H}=f_V\frac{1-\epsilon_H}{1+2\epsilon_H}+(1-f_V)\frac{\epsilon-\epsilon_H}{\epsilon+2\epsilon_H}, \tag{1}$$

where ϵ_H is the dielectric function of the "host" material. If ϵ_H equals 1, $\langle\epsilon\rangle$, or ϵ, then Eq. (1) reduces to the Lorentz-Lorenz (LL),[43] Maxwell-Garnett (1) (MG1),[44] Bruggeman effective-medium approximation (EMA),[45] or Maxwell-Garnett (2) (MG2) model,[44] respectively. Here, the MG1 or MG2 notation refers to the Maxwell-Garnett formalism with the host dielectric chosen to be void ($\epsilon_H=1$) or medium ($\epsilon_H=\epsilon$), respectively. We use here the EMA ($\epsilon_H=\langle\epsilon\rangle$) because it treats both void and material phases on an equal, self-consistent basis, and was shown to give the best effective-medium description of surface roughness over an extended spectral range for amorphous silicon.[41] We shall show in Sec. III C that the LL and MG1 models also can be excluded here on the basis of the observed spectral line shapes given in Figs. 1 and 2.

Solutions of Eq. (1) for $\langle\epsilon\rangle$ for various void concentrations are shown in Fig. 4. Here, the solid-line spectrum of Fig. 1 was used for ϵ. For small void fractions, the lineshapes of both ϵ_1 and ϵ_2 are preserved and the $\langle\epsilon\rangle$ spectra simply scale between their homogeneous limits ϵ and $\epsilon_{\text{void}}=1+i0$. The scaling property can be shown explicitly by expanding Eq. (1) to first order for $f_V<<1$. Both EMA and MG2 theories yield

$$\langle\epsilon\rangle\cong\epsilon\left(1-3f_V\frac{\epsilon-1}{2\epsilon+1}\right), \tag{2a}$$

$$\cong\epsilon(1-\tfrac{3}{2}f_V), \tag{2b}$$

where Eq. (2b) follows if either $|\epsilon|>>1$ or $\epsilon_2>>|\epsilon_1|$, as is the case here.

For void volume fractions larger than 0.5, the ϵ_1 and ϵ_2 line shapes become mixed and the simple scaling approach is not valid. After first decreasing, the values of ϵ_2 in the Drude region begin to increase and finally to exceed the original values for the homogeneous material. Lifetime broadening

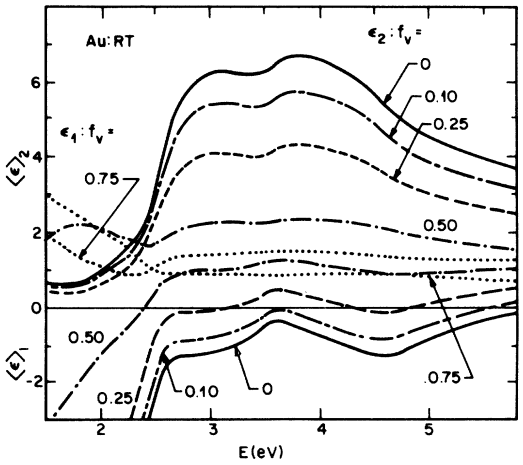

FIG. 4. Effect of increasing void fraction on the apparent dielectric function of Au, calculated in the EMA by Eq. (1).

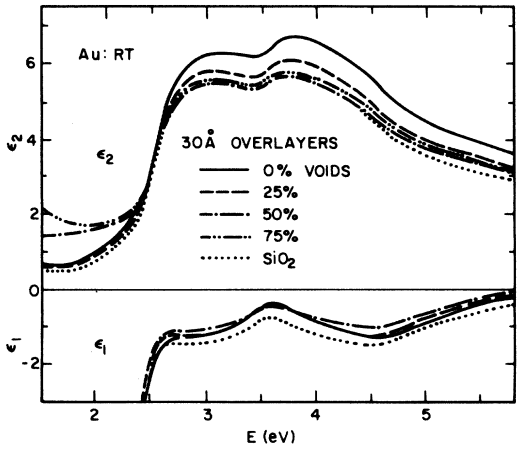

FIG. 5. Effect of varying degrees of surface roughness on the apparent dielectric function, calculated by assuming 30 Å thick overlayers of EMA void fractions as indicated. A spectrum calculated for a 30 Å SiO_2 overlayer simulating organic contamination is also shown.

effects also act to increase ϵ_2 in this region, as will be discussed in Sec. III D. However, lifetime effects can be distinguished from the effective-medium increase by examining the interband region above 2.5 eV. The appearance of an absorption band below the 2.5 eV main structure for $f_V = 0.5$ is reminiscent of the "anomalous absorption" band seen by Thèye[14] and attributed to impurities.

The effect of surface roughness can be simulated by effective-medium overlayers.[41] The effects for 30 Å overlayers of various values of f_V on homogeneous substrates are shown in Fig. 5. Overlayers increase ϵ_1 and decrease ϵ_2 in a manner similar to that calculated for small volume fractions of voids, with a change in both ϵ_1 and ϵ_2 in the interband region that is almost independent of the actual void fraction in the overlayer. However, for large void fractions ϵ_2 is increased in the Drude region because of the mixing effect shown in Fig. 4.

By contrast to the effect of roughness, a dielectric overlayer lowers both ϵ_1 and ϵ_2 curves, as also shown in Fig. 5. We used the dielectric function for SiO_2 for this computation because it is similar to those of a wide range of organic contaminants and has been conveniently approximated in simple analytic form.[47]

C. Interband region: $E > 2.5$ eV

Figures 1 and 2 show that structure in the interband region is remarkably insensitive to preparation or annealing, as noted previously by Winsemius, Lengkeek, and Van Kampen.[24] The ϵ_2 spectra qualitatively differ only by scaling factors, as given approximately by Eq. (2b). This suggests immediately that differences in ϵ_2 spectra in this spectral range are determined primarily by the amount of polarizable material per unit volume, or void fraction,[8] as opposed to scattering by defects[1,2,4,14] or grain boundaries,[24,28] or by internal strain.[1,2,24] Scattering and strain would broaden intrinsic structure but would not affect average amplitudes, by contrast to the results shown in Figs. 1 and 2.

However, a void model can apply only if the grains comprising the polarizable fraction of the heterogeneous material retain their spectral identity to the smallest sizes encountered. Self-consistent molecular-orbital calculations for Cu by Messmer, *et al.*,[48] show that the essential features of a band picture, that is, narrow 3*d* bands and broad 4*s* bands that overlap them, are already well developed in cubo-octahedral clusters containing 13 atoms. The separation of energy levels in the 4*s* bands of well-isolated, regular clusters is estimated to be of the order of $E_F/N^{2/3}$, where $E_F \cong 5.50$ eV is the Fermi energy of gold and N is the number of atoms in a cluster.[49] Thus 30 Å clusters, for which $N \cong 1000$, would have an effective continuum of levels and by both measures would appear as bulk material with respect to interband transitions. The minimum grain sizes shown in Fig. 3 are comfortably over this limit, whence a scaling behavior or ϵ_2 in the interband region is not surprising. We also note that grains imply voids, because it is impossible to produce grain boundaries in fcc or hexagonal close-packed lattices without losing density.

Comparisons between the predictions of Eq. (1) and the data of Fig. 1 are shown in Fig. 6, where

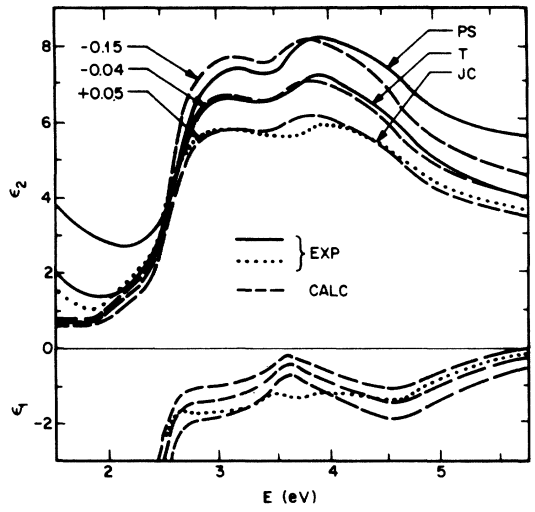

FIG. 6. Comparison of selected experimental spectra from Fig. 1 with one-parameter calculated spectra. The calculated spectra were obtained from the electron-beam deposited sample data of Fig. 1 by assuming different void fractions within the EMA as shown.

we have used as ϵ the data of Fig. 2 for the electron-beam-deposited sample. This reference sample was deposited at room temperature. By Fig. 3b, it will have numerous grain boundaries and therefore voids. However, we choose its spectrum as reference because of its small Drude tail. Negative values of f_V that may result by using this spectrum for ϵ in Eq. (1) simply mean that the compared data were obtained on material more dense than the reference film. Positive values of f_V correspond to more loosely packed films.

Line shapes calculated from Eq. (1) for values $f_V = -0.15$, -0.04, and $+0.05$ compare well to the Pells-Shiga,[21] Thèye,[14] and Johnson-Christy[15] data, as shown in Fig. 6. Thus a single parameter is sufficient to describe differences among ϵ_2 spectra over the entire interband range. The Winsemius data are not shown but correspond to a value $f_V \cong 0.03$. Taken at face value, these results indicate that material density increases in sequence with unannealed thin films, heavily annealed bulk polycrystalline material, electron-beam evaporated moderately thick films, annealed thin films, and annealed bulk polycrystalline material. The decrease of void fraction of Au films with annealing is well known[19] and can be seen also in Fig. 3, and thus the trend of the data is entirely reasonable with the apparent exception of the Winsemius results. But Winsemius has noted[24,25] that the annealing process results in thermal etching, or grooving.[50] The effect of such surface roughness would be to decrease ϵ_2 in the interband region while increasing it in the Drude region, as seen in Fig. 5. Thus our interpretation of the Winsemius data is that the surfaces were rough.

In the annealing context, Johnson and Christy[15] noted that one annealed sample which they had measured gave results essentially identical to those of Thèye.[14] They rejected both data on the basis that the samples were too thin. However, Fig. 6 shows that both types of data are characteristic of the preparation method, and that the unannealed Johnson-Christy films simply contained more voids.

Quantitative comparisons of the one-parameter model were obtained for the TEM-characterized data of Fig. 2 by using linear regression analysis.[40] $\langle\epsilon\rangle$ spectra calculated from Eq. (1) in the EMA were least-squares fitted to both ϵ_1 and ϵ_2 at 62 points over the energy range 2.5–5.8 eV for all three samples. The results for the liquid-N_2 sample are shown in Fig. 7. Using f_V as the single free parameter, we find that $f_V = 0.21 \pm 0.01$, where the uncertainty represents the 90% confidence level based on the fit of the model to the data. The unbiased estimator, $\hat{\sigma}$, of the mean-square deviation, δ, is 0.23.

The results are seen to give a good representation of *both* ϵ_1 and ϵ_2 over the entire interband range. The ability to retain structure and to match ϵ_1 while simultaneously reproducing ϵ_2 over an extended spectral range constitutes the real test of the one-parameter model and shows that voids indeed explain the major spectral differences in this range. The void fraction of $21 \pm 1\%$ exceeds the clear area fraction of 12% from Fig. 3(a), as expected from the three-dimensional nature of void distribution.

Similar results for the RT and 250 C films are shown in Figs. 8 and 9, respectively. The void fractions are 0.04 ± 0.01 and 0.01 ± 0.01, and the $\hat{\sigma}$ values are 0.33 and 0.32, respectively. Although

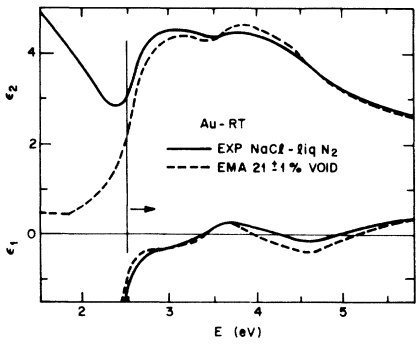

FIG. 7. Comparison of liquid-N_2 thin-film sample spectra from Fig. 2 with a one-parameter EMA calculation assuming 21% voids.

density estimates were not possible from TEM micrographs, the optical data show that the large-grain 250°C sample is more dense than the small-grain RT sample, as expected from grain boundary considerations.

A close examination of Figs. 8 and 9 shows that the experimental value of ϵ_1 lies below the calculated value, meaning that the best fit is a compromise between ϵ_1 and ϵ_2. Figure 5 shows that this behavior is characteristic of a dielectric overlayer. To improve the fit, we therefore generalized the model to include a dielectric overlayer simulated by the analytic expression for the refractive index of SiO_2.[47] Such overlayers are present if the films have been exposed to air, as was the case here and also for many data reported in the literature. The results are also shown in Figs. 8 and 9 for the RT and 250°C samples. The two-parameter model yields $f_V = 0.00 \pm 0.01$, $d = 14 \pm 2$ Å, and $\hat{\sigma} = 0.14$ for the RT sample, and $f_V = -0.02 \pm 0.01$, $d = 13 \pm 2$ Å, and $\hat{\sigma} = 0.15$ for the 250°C sample.

Thus the two-parameter model improves the fit by a factor of 2 and causes small adjustments in the absolute values of the void fractions. We note that the new void fraction for the RT sample is just equal to that for the reference sample, which was also deposited on a room-temperature substrate, and the 250°C sample is slightly more dense.

We comment finally on the Lorentz-Lorenz approximatimation, which is obtained from Eq. (1) by setting $\epsilon_H = 1$. Expanding the resulting expression to first order in $f_V \ll 1$ yields

$$\langle\epsilon\rangle \cong \epsilon\left(1 - f_V \frac{(\epsilon - 1)(\epsilon + 2)}{3\epsilon}\right), \tag{3}$$

which is the LL analog of Eq. (2b). If $\epsilon_2 \gg |\epsilon_1|$, the correction term is nearly imaginary and the line shapes ϵ_1, ϵ_2 of ϵ become mixed. Thus for small f_V the imaginary part of $\langle\epsilon\rangle$ will hardly change, while the real part will increase substantially. Figures 1 and 2 show that this behavior is not seen experimentally. We conclude in agreement with previous results on microscopically rough amorphous Si films,[41] and consistent with the meaning of the approximation, that the Lorentz-Lorenz model is not applicable in this limit.

D. Drude region: $E < 2.5$ eV

Analysis of ϵ_2 data in the Drude region is complicated by the fact that at least two mechanisms contribute to increasing ϵ_2 above the intrinsic bulk value. It is intuitively obvious that ϵ_2 will increase whenever the grain size drops below the 380 Å intrinsic mean free path, because the lifetime will be shortened and the Drude tail broadened into the near ir. We note that the characteristic sample length for the Drude region, i.e., the mean free path, is more than an order of magnitude larger than that for the interband region, and thus the intraband region is more sensitive to microscopic sample quality. The liquid-N_2 sample of Fig. 2 shows broadening from this mechanism. The void fraction does not influence ϵ_2 significantly, except for the scattering introduced, but it decreases the magnitude of ϵ_1 through the dependence of the plasma frequency on electron volume density.

Less easy to identify unambiguously is the effect of surface roughness, which generally has been assumed to give rise to all Drude tail enhancement.[14,24,29] Roughness acts both to decrease the effective mean free path through increased surface scattering and also to provide an apparent increase in ϵ_2 through the Fresnel reflectance equations simply by acting as an effective medium on the surface, as shown in Fig. 5. The surface scattering mechanism has been discussed in detail by Thèye.[14] The strongest evidence for the existence

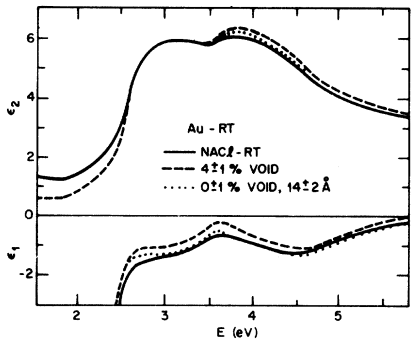

FIG. 8. Same as Fig. 7, but for the RT thin-film sample of Fig. 2. Also shown are the results of a two-parameter calculation assuming voids and an overlayer film.

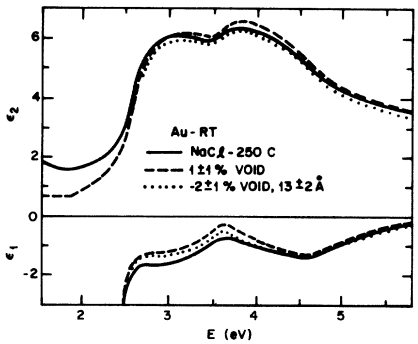

FIG. 9. Same as Fig. 8, but for the 250 °C sample of Fig. 2.

of surface roughness mechanisms is that the ϵ_2 spectrum shows a clear minimum in the Drude region for all samples prepared on room-temperature substrates, as shown in Fig. 1. Even though the grain sizes in RT samples are much smaller than those of annealed material, leading to a shorter mean free path, nevertheless ϵ_2 is invariably smaller for RT samples than for annealed material. The connection to surface roughness follows immediately because samples are known to groove upon annealing.[50]

The lower limit on ϵ_2 in the Drude region can be calculated from the simple theory of the dielectric response of a free-electron gas.[14] If τ is the carrier lifetime, then

$$\epsilon_2 = \omega_p^2/\omega^3\tau \,, \tag{4}$$

where $E_p = \hbar\omega_p = 9.33$ eV is the plasma energy.[14] Using the value $\tau = 2.7\times10^{-14}$ sec as calculated from 295-K resistivity data on pure bulk crystals[35] and assuming that the conduction mass equals the free-electron mass, it follows that the minimum value of ϵ_2 at 1.5 eV due to zero frequency scattering is 0.6. At finite frequencies the electron-electron scattering contribution increases as[51]

$$\tau_{ee}^{-1}(\omega) = \tau_{ee}^{-1}(0) + \frac{\omega^2}{4\pi^2\omega_p} \,, \tag{5}$$

while the electron-phonon scattering contribution remains constant. Even if electron-electron scattering dominated, ϵ_2 would only increase by 0.16 at 1.5 eV. Thus, ϵ_2 theoretically should by ~0.6–0.8, which by Fig. 1 is about half the value attained in previous measurements.

However, this calculated limit compares very well with data that we have taken on moderately thick ($d \cong 1500$ Å) Au films electron beam evaporated on MaCl and glass substrates, as shown in Fig. 1. These data yield an ϵ_2 value between 0.7 and 1.1 at 1.5 eV, indicating that these samples are of higher overall quality than those previously used to study the Drude region, even though they have a smaller grain size than annealed samples.

One consequence of excessive scattering is to mask the interband transition threshold of Au, as can be seen from the ϵ_2 spectra of Fig. 2. The solid curve is a measured spectrum that defined the lower boundary of experimental uncertainty in Fig. 1. The threshold for d-band to Fermi-level transitions, which occurs first near X in the Brillouin zone,[52,53] is seen clearly at 1.84 eV in Fig. 2. The line shape for ϵ_2 for this region has been investigated extensively in the one-electron approximation by Guerrisi, Rosei, and Winsemius[25] (GRW) in simplified model calculations based on the band structure obtained by Christensen and Seraphin.[52] GRW showed that it should increase linearly from threshold. Thus the data shown in Fig. 2 verify in a very direct manner the theoretical predictions of GRW.

The existence of a rather large Drude tail obscuring the threshold prevented GRW from obtaining an accurate estimate of the threshold energy. Using data from Winsemius,[25] the edge was calculated to be 1.94 eV, but using data from Thèye[14] the edge was found to occur at 1.82 eV. Our data show the latter result to be more nearly correct.

The connection between increased values of ϵ_2 in the Drude region and grain size in samples with a large volume fraction of imperfections can be made quantitative by the recent work of Kreibig[54] on ϵ_2 values of fine Au particles of approximately uniform size dispersed in glass matrices. Values of ϵ_2 at the plasma resonance maximum of 5100 Å in this system showed a strictly linear dependence on reciprocal particle diameter over the measurement range of 100 Å, where $\epsilon_2 \cong 3.4$, to 20Å, where $\epsilon_2 \cong 8.3$. The value for bulk Au at 5100 Å extrapolated to $\epsilon_2 \cong 2.1$, in agreement with data shown for good samples in Fig. 1. The dependence on reciprocal diameter is easily understood if the scattering length is proportional to the diameter. Using $\Lambda = v_F\tau$, where the Fermi velocity $v_F = 1.5\times10^8$ cm/sec for Au, it follows that Eq. (4) must have added to it an additional term:

$$\epsilon_{2s} = \omega_p^2 v_F/\omega^3\Lambda \,, \tag{6}$$

which has the correct form if $\Lambda \sim d$, where d is the particle diameter.

From previous measurements on Ag, Kreibig showed[55] that the constant of proportionality is such that $\Lambda = r$, where r is the particle radius. This result implies isotropic scattering at grain surfaces. Although the calculation was not performed for Au, it is straigthforward to show from the data of Ref. 54 that at 5100 Å, $\Lambda \cong 9$ Å for a 20 Å diameter particle. Thus taking Λ to be equal to the particle radius for spherical particles appears to be valid also for Au.

For nonspherical or irregularly shaped grains, or grains that themselves contain grain boundaries, there is no reason to suppose that Λ can be identified with any single dimension. But nevertheless it is useful to evaluate Λ from ϵ_2 data. Using Eq. (6) with 1.5 eV values it follows that

$$\Lambda \cong 240 \text{ Å}/[\epsilon_2(1.5 \text{ eV}) - 0.8] \,. \tag{7}$$

For the data sources shown in Fig. 1, we find that Λ equals 200, 340, 160, and 80 Å for the data of Thèye,[14] Johnson and Christy,[15] Winsemius,[25] and Pells and Shiga,[21] respectively. Both Thèye and Johnson and Christy obtained their results on films about 200 Å thick, the difference being that Thèye's films were annealed and the Johnson-

Christy films were not. We conclude from these data that the annealing process causes surface roughening, with a resultant increase in the amount of surface scatter. By this criterion the well annealed bulk samples of Winsemius[25] and Pells and Shiga[21] were considerably rougher, a result consistent with grooving studies of polycrystalline systems.

IV. CONCLUSIONS

We have shown that the major discrepancies in above-band-gap reported dielectric-function data for Au can be explained in a one-parameter model that incorporates voids in otherwise homogeneous material. The model has been examined quantitatively for data from films deposited on NaCl at various temperatures and characterized independently by TEM. In the below-band-gap region, we have shown that data on moderately thick samples reproduce within experimental error the value of ϵ_2 calculated from intrinsic scattering as determined from known resistivity values and the dependence of scattering on frequency, by contrast to previous work which showed ϵ_2 values at least a factor of 2 higher. The moderately thick sample data verified directly the linear threshold model calculations of Guerisi, Rosei, and Winsemius,[25] and allowed an unambiguous determination of the threshold at 1.84 eV at 295 K.

However, the "real" dielectric function of Au is still undetermined. Sample preparation is of primary importance, while the optical measurement technique makes little difference. It is discouraging to note that the conditions yielding the best data in the Drude and interband regions are mutually exclusive; that is, samples should not be annealed in the former case but should be annealed in the latter case. Preparation of epitaxial thin-film samples in ultrahigh vacuum may provide a way out of this dilemma. Measurements on such samples should be performed *in situ* to eliminate possible surface film effects.

It is not clear that bulk samples will yield better data than thin-film samples. Our results with unannealed films about 1500 Å thick show better microscopic quality in the Drude region. But the Pells-Shiga data[21] on annealed bulk material, if taken at face value, show a much lower void fraction from interband values of ϵ_2 than anything previously reported. Thèye[14] has discussed these data and rejected them on the basis of instrumentation problems, but we believe that the issue has not yet been resolved satisfactorily.

The determination of accurate dielectric function data for Au would be of interest not only in its own right, but also as a means of assessing independently and conveniently sample quality by optical means. The effect of voids and grain boundaries, with the concomitant increase in surface area relative to apparent values, can be particularly severe in experiments involving adsorption. Further, the tendency of voids and grain boundaries to concentrate optical fields should also be important in surface Raman scattering. Finally, the analytic approach taken here should be useful in analysis of optical spectra of other metals, which tend to show much wider variation in reported optical properties than do those of Au.

ACKNOWLEDGMENT

We thank C. Doherty for preparing the electron-beam evaporated samples used in these measurements, and S. Nakahara for taking the TEM micrographs.

[1]L. Schulz, J. Opt. Soc. Am. 44, 357 (1954).
[2]L. Schulz and F. Tangherlini, J. Opt. Soc. Am. 44, 362 (1954).
[3]L. R. Canfield, G. Hass, and W. R. Hunter, J. Phys. (Paris) 25, 124 (1964).
[4]H. Mayer and H. Bohme, J. Phys. 25, 81 (1964).
[5]D. Beaglehole, Proc. Phys. Soc. London 85, 1007 (1965).
[6]D. Beaglehole, in *Optical Properties and Electronic Structure of Metals and Alloys*, edited by F. Abeles (North-Holland, Amsterdam, 1966), p. 154.
[7]H. E. Bennett and J. M. Bennett, in Ref. 6, p. 175.
[8]J. Hodgson, J. Phys. Chem. Solids 29, 2175 (1968).
[9]D. Beaglehole and E. Erlbach, Solid State Commun. 8, 255 (1970).
[10]G. B. Irani, T. Huen, and F. Wooten, Phys. Rev. B 6, 2904 (1972).
[11]L. G. Schulz, J. Opt. Soc. Am. 44, 540 (1954).
[12]H. Fukutani and O. Sueoka, in Ref. 6, p. 565.
[13]P. O. Nilsson, Phys. Kondens. Mater. 11, 1 (1970).
[14]M.-L. Thèye, Phys. Rev. B 2, 3060 (1970).
[15]P. B. Johnson and R. W. Christy, Phys. Rev. B 6, 4370 (1972).
[16]H.-J. Hagemann, W. Gudat, and C. Kunz, J. Opt. Soc. Am. 65, 742 (1975); DESY Report No. SR-74/7 (unpublished).
[17]M. Otter, Z. Phys. 161, 163 (1961).
[18]B. Dold and R. Mecke, Optik. 22, 435 (1965).
[19]W. Köster and R. Stahl, Z. Metallk. 58, 768 (1967).
[20]E. Meyer, H. Frede, and H. Knof, J. Appl. Phys. 38, 3682 (1967).
[21]G. P. Pells and M. Shiga, J. Phys. C 2, 1835 (1969).
[22]G. Jungk, Phys. Status Solidi A 3, 965 (1970).
[23]D. E. Aspnes, Opt. Commun. 8, 222 (1973).

[24]P. Winsemius, H. P. Lengkeek, and F. F. Van Kampen, Physica (The Hague) 79B, 529 (1975).
[25]M. Guerrisi, R. Rosei, and P. Winsemius, Phys. Rev. B 12, 557 (1975).
[26]G. Jungk and R. Gründler, Phys. Status Solidi B 76, 541 (1976).
[27]R. Kirsch, Phys. Status Solidi A 46, 459 (1978).
[28]O. Hunderi, Phys. Rev. B 7, 3419 (1973).
[29]M. L. Thèye, Phys. Lett. A 25, 764 (1967).
[30]O. Hunderi and H. P. Myers, J. Phys. F 3, 683 (1973).
[31]S. R. Nagel and S. E. Schnatterly, Phys. Rev. B 9, 1299 (1974).
[32]See, e.g., S. Norrman, T. Andersson, C. G. Granqvist, and O. Hunderi, Phys. Rev. B 18, 674 (1978), and references therein; and P. O'Neill and A. Ignatiev, Phys. Rev. B 18, 6540 (1978), and references therein.
[33]T. E. Furtak and J. Reyes, Surf. Sci. (in press).
[34]P.-O. Nilsson, Solid State Phys. 29, 139 (1974).
[35]*American Institute of Physics Handbook*, 3rd ed., edited by D. E. Gray (McGraw-Hill, New York, 1972), pp. 9–39.
[36]H. C. Theurer and J. J. Hauser, J. Appl. Phys. 35, 554 (1964).
[37]J. S. Vermak and C. A. O. Henning, Philos. Mag. 22, 269 (1970); J. N. Orcheson, F. W. Boswell, J. M. Corbett, and C. A. O. Henning, Thin Solid Films 51, 395 (1978).
[38]D. E. Aspnes and A. A. Studna, Appl. Opt. 14, 220 (1975); Proc. Soc. Photo-Opt. Instrum. Eng. 112, 62 (1977); Rev. Sci. Instrum. 49, 291 (1978).
[39]D. E. Aspnes, J. Opt. Soc. Am. 64, 812 (1974).
[40]E. S. Keeping, *Introduction to Statistical Inference* (Van Nostrand, Princeton, 1962), Chap. 12.
[41]D. E. Aspnes, J. B. Theeten, and F. Hottier, Phys. Rev. B 20, 3292 (1979).
[42]D. E. Aspnes, J. B. Theeten, and R. P. H. Chang, J. Vac. Sci. Technol. 16, 1374 (1979).
[43]C. G. Grandqvist and O. Hunderi, Phys. Rev. B 16, 3513 (1977).
[44]J. C. M. Garnett, Philos. Trans. R. Soc. London 203, 385 (1904); Sec. A 205, 237 (1906).
[45]D. A. G. Bruggeman, Ann. Phys. (Leipzig) 24, 636 (1935).
[46]R. M. A. Azzam and N. M. Bashara, *Ellipsometry and Polarized Light* (North-Holland, Amsterdam, 1977).
[47]See Ref. 35, p. 6–29.
[48]R. P. Messmer, S. K. Knudson, K. H. Johnson, J. B. Diamond, and C. Y. Yang, Phys. Rev. B 13, 1396 (1976).
[49]R. Kubo, *Polarisation, Matière et Rayonnement*, Vol. Jubilaire en l'Honneur D. A. Kastler (Presse, Paris Université de France, 1969).
[50]P. G. Shewmon, *Diffusion in Solids* (McGraw-Hill, New York, 1963), p. 179.
[51]R. N. Gurzhi, Zh. Eksp. Teor. Fiz. 35, 965 (1958) [Sov. Phys. JETP 8, 673 (1959)].
[52]N. E. Christensen and B. O. Seraphin, Phys. Rev. B 4, 3321 (1971).
[53]J. D. E. McIntyre and W. F. Peck, Jr., in *Proceedings of the Symposium on Electrocatalysis*, edited by M. W. Breiter (Electrochemical Society, Princeton, 1974), p. 212.
[54]U. Kreibig, Solid State Commun. 28, 767 (1978).
[55]U. Kreibig, J. Phys. F 4, 999 (1974).

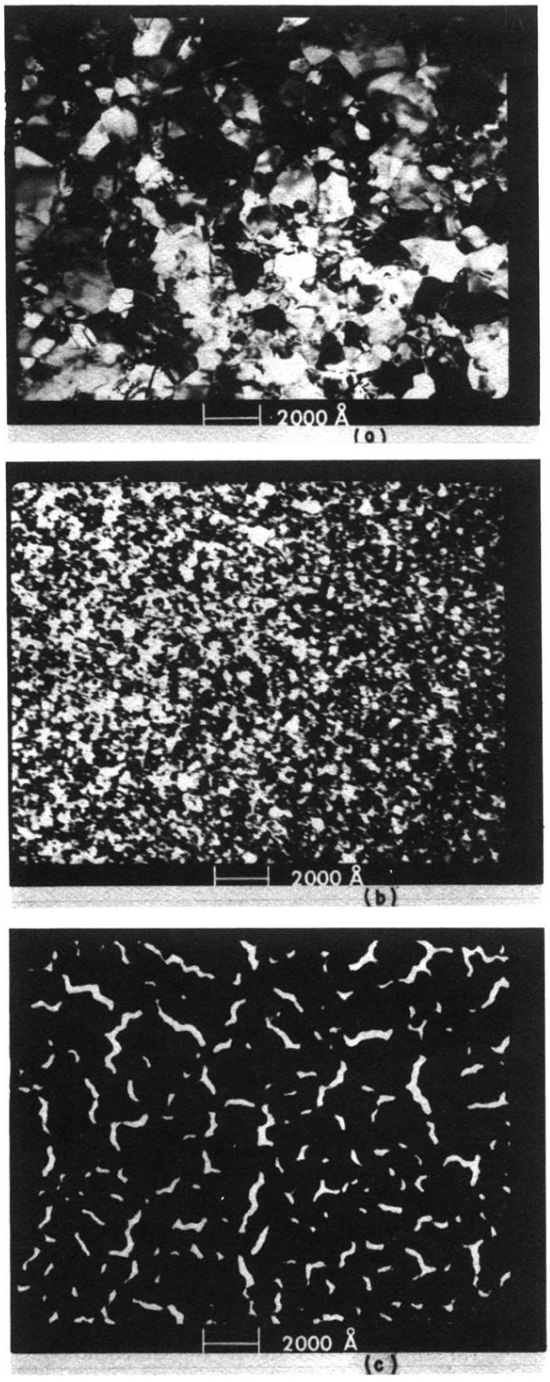

FIG. 3. TEM micrographs of sputter-deposited thin films whose dielectric function data are shown in Fig. 2. (a) 250 °C; (b) RT; (c) liquid N_2.